Spectroscopic studies of the Chan-Lam amination: A mechanism-inspired solution to boronic ester reactivity

Julien C. Vantourout,[a,b] Haralampos N. Miras,[c] Albert Isidro-Llobet,[b] Stephen Sproules,[c] and Allan J. B. Watson[a]*

[a] Department of Pure and Applied Chemistry, WestCHEM, University of Strathclyde, Glasgow, G1 1XL, UK.

[b] GlaxoSmithKline, Medicines Research Centre, Gunnels Wood Road, Stevenage, SG1 2NY, UK.

[c] School of Chemistry, WestCHEM, University of Glasgow, Glasgow G12 8QQ, UK.

ABSTRACT: We report an investigation of the Chan-Lam amination reaction. A combination of spectroscopy, computational modeling, and crystallography has identified the structures of key intermediates and allowed a complete mechanistic description to be presented, including off-cycle inhibitory processes, the source of amine and organoboron reactivity issues, and the origin of competing oxidation/protodeboronation side reactions. Identification of key mechanistic events has allowed the development of a simple solution to these issues: manipulating Cu(I)→Cu(II) oxidation and exploiting three synergistic roles of boric acid has allowed the development of a general catalytic Chan-Lam amination, overcoming long-standing and unsolved amine and organoboron limitations of this valuable transformation.

1. INTRODUCTION

Transition metal-mediated C-N bond formation is an essential transformation that enables the preparation of valuable aryl amine products.[1] Copper-catalyzed processes such as the Ullmann[2] and Chan-Lam[3,4] reactions are both particularly valuable and widely practiced (Scheme 1). The Ullmann reaction has seen significant development, particularly in the context of ligand design to allow milder reaction conditions and overcoming reactivity issues with aryl chloride electrophiles.[5] Where the Ullmann reaction follows the characteristic transition metal-catalyzed nucleophile/electrophile coupling, the Chan-Lam amination is unique, coupling two nucleophiles, an aryl organoboron compound and an amine, usually under mild oxidative conditions (air or O_2).[4]

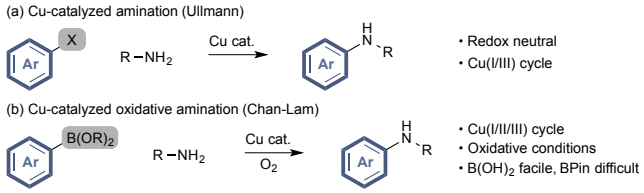

Scheme 1. Cu-catalyzed C-N bond formation.

2. GOALS OF THIS STUDY

A major limitation of the Chan-Lam amination has been the lack of general reactivity using aryl boronic acid pinacol (BPin) esters, especially with aryl amines.[6] While conversion of BPin to the boronic acid is relatively straightforward,[7] aryl BPin are more readily accessed, especially by modern transition metal-catalyzed methodologies.[8] In addition, BPin are often more stable than boronic acids, where protodeboronation can be problematic for several substrate classes.[9] There have been several approaches to improving aryl BPin reactivity, including the use of additives to achieve boron species interconversion *in situ* and the use of substrates bearing Cu-ligating groups that are seemingly more reactive.[6,10]

The origin of these reactivity differences is unknown and a purely steric argument was unsatisfactory: Chan-Lam-type amination of specific BPin species have been reported[10] and aryl BPin are competent in numerous other transition metal-catalyzed reactions.[7] More broadly, the utility of the Chan-Lam amination is hampered by significant problems with byproduct formation and the mechanism of the amination remains elusive,[11] although a seminal study of the related etherification process by Stahl has provided a solid foundation for understanding these Cu-based oxidative coupling reactions.[12]

Here we report a spectroscopic investigation of the Chan-Lam amination reaction, providing a complete mechanistic description, including off-cycle inhibitory processes, the source of amine and organoboron substrate reactivity issues, and the origin of competing oxidation/protodeboronation side reactions. This knowledge has been leveraged to provide a simple solution to the catalytic Chan-Lam amination of both boronic acids and BPin esters with alkyl and aryl amines.

3. PREVIOUS WORK

Seminal studies by Stahl have provided key insight into the mechanism of the related etherification process, using a boronic acid dimethyl ester in MeOH as the benchmark process (summarized in Scheme 2).[12]

Stahl's process begins from a Cu(II) species (**1**) that undergoes transmetallation with boronic ester **2** to deliver aryl Cu(II) species **4**, releasing byproduct **3**. Stahl proposed **9** as a resting state with turnover-limiting transmetallation proceeding via **10**. Oxidation of **4** to Cu(III) complex **6** occurs via disproportionation with a second equivalent of **1**, liberating Cu(I) complex **5**. Reductive elimination of ether product **7** gives **5**, which is reoxidized to **1** using O_2, HX, and X–$B(OMe)_2$ to complete the cycle. While there are several fundamental differences between the etherification process and the amination reaction, this key study provides important data that proved highly informative for assembling a complete mechanistic description of the amination reaction (*vide infra*).

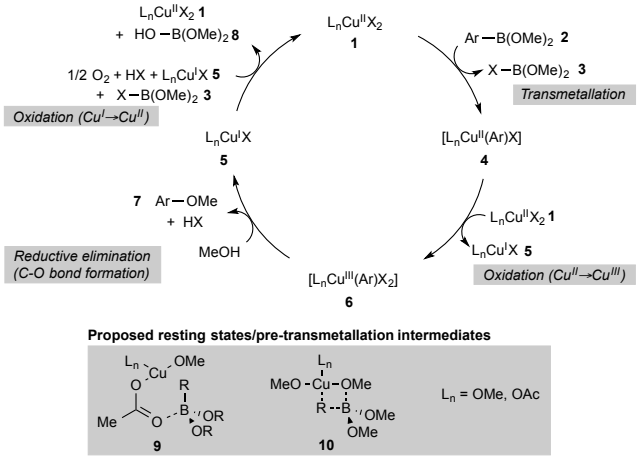

Scheme 2. Summarized version of Stahl's etherification mechanism and proposed catalyst resting states/pre-transmetallation intermediates.

4. RESULTS

4.1 Reaction Profiles and Identification of Byproducts. Control experiments were performed to evaluate the performance of the Chan-Lam amination using representative members of two amine classes, piperidine (**12**, alkyl) and aniline (**14**, aryl), and two organoboron compounds, boronic acid (**11a**) and BPin ester (**11b**).

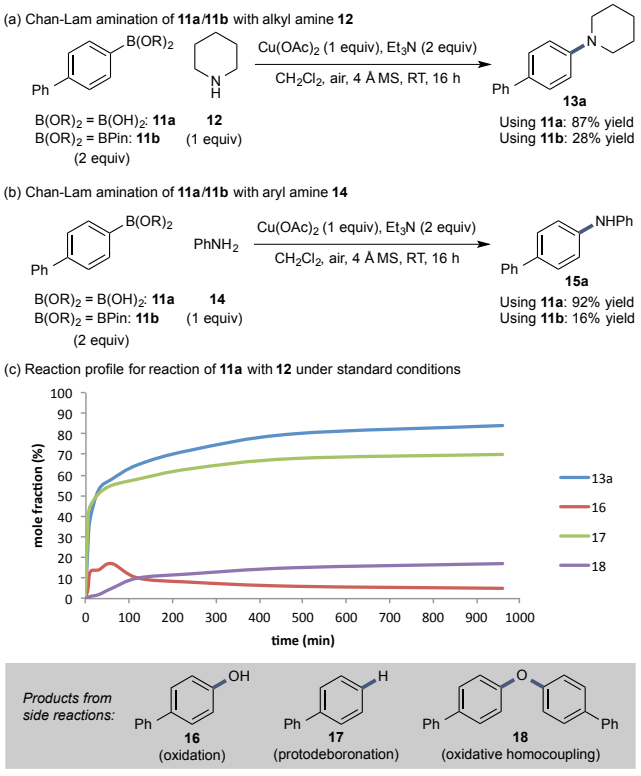

Scheme 3. Standard conditions: organoboron compound (2 equiv), amine (1 equiv, 0.20 mmol), $Cu(OAc)_2$ (1 equiv), Et_3N (2 equiv), 4 Å MS in DCM (0.25 M), RT, 16 h. (a) Reaction of **11a** and **11b** with **12**. Isolated yields. (b) Reaction of **11a** and **11b** with **14**. Isolated yields. (c) Reaction profile of the amination of **11a** with **12**. Determined by HPLC analysis.

Under standard conditions (1 equiv amine, 2 equiv organoboron reagent, 1 equiv $Cu(OAc)_2$; see Scheme 3 and ESI) using **12** as the amine coupling partner (Scheme 3a), boronic acid **11a** is converted to product **13a** in 87% yield while the corresponding BPin **11b** provides 28% yield. Using **14** as the amine component with **11a** gives product **15a** in 92% yield and 16% yield using **11b** (Scheme 3b).

Several byproducts were identified including phenol **16**, protodeboronation product **17**, and oxidative homocoupling product **18**.[3,4,11] A reaction profile for the reaction in Scheme 3a is given in Scheme 3c. Protodeboronation was comparable to amination, while competing oxidation delivers **16** and, as [**16**] increases, competing Cu-catalyzed etherification delivers **18**.

Table 1 provides the full product distribution for the reaction of amines **12** and **14** with **11a**. These values are based on the organoboron reagent (2 equiv vs. 1 equiv amine) in order to fully appraise the extent of byproduct formation.

Table 1. Product distribution in the amination of boronic acid **1a** with piperidine (**12**) and aniline (**14**).[a]

		SM	Product[b]	Byproducts[c]		
Entry	**Et_3N** (equiv)	**11a** (%)[b]	**13a/15a** (%)[b]	**16** (%)[b]	**17** (%)[b]	**18** (%)[b]
Using amine **2**:						
1	0	32	66	1	51	21
2	1	2	76	7	67	25
3	2	2	87	6	68	16
4[d]	2	2	65	45	65	12
5	3	3	97	13	62	13
Using amine **4**:						
6	0	46	46	1	61	22
7	1	12	69	7	67	20
8	2	8	92	4	65	15
9[d]	2	3	60	51	50	15
10	3	1	93	10	67	13

[a] Reagents and conditions from Scheme 3 unless otherwise stated. [b] Isolated yields. [c] Determined by HPLC analysis. [d] Reaction without 4 Å MS.

Under especially dry reaction conditions, the quantity of **16** and **18** can be lowered significantly and homocoupling of the organoboron component can be observed, giving tetraphenyl **19** (Scheme 4).[10d,e,13] Homocoupling was only observed under atypical (strictly anhydrous) reaction conditions and was significantly less problematic than oxidation and protodeboronation.

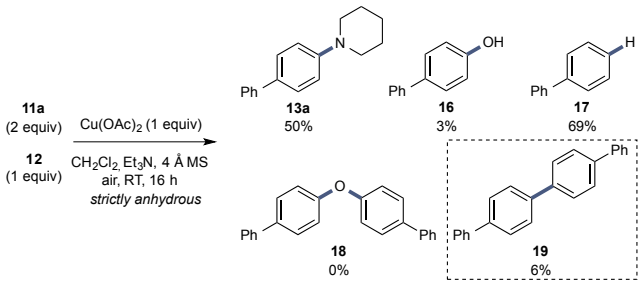

Scheme 4. Observation of organoboron homocoupling**.** Isolated yields.

4.2 Assessment of Inhibitors. The addition of AcOH and AcOK has been observed to inhibit the related etherification process.[12] The reactions of amines **12** and **14** with boronic acid **11a** were assessed in the presence of added AcOH, AcOK, as well as pinacol in order to probe any inhibitory effects and assist in establishing similarities with the etherification reaction (Figure 1).

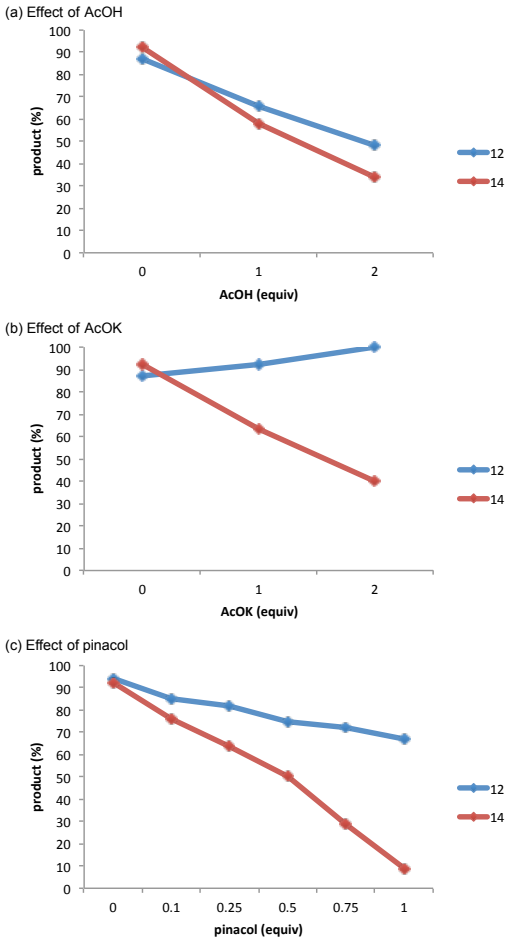

Figure 1. Effect of addition of (a) AcOH, (b) AcOK, and (c) pinacol to the Chan-Lam amination of **11a** with **12** (blue line) and **14** (red line) under standard conditions. Determined by HPLC.

AcOH inhibited the amination of both **12** and **14** (Chart a). AcOK inhibited only the reaction of **14** (Chart b, red line) and was found to be beneficial to efficiency for the reaction using **12** (Chart b, blue line). Pinacol was found to inhibit both amination reactions, with a stronger effect on the reaction of **14** than that of **12** (Chart c).

4.3 Identification and Analysis of Cu(II) Complexes. *4.3.1 EPR Analysis of Paddlewheel Dissociation.* $[Cu(OAc)_2]_2•2H_2O$ is used as standard in the majority of Chan-Lam amination reactions.[3,4] The effect of the amine and organoboron components on $[Cu(OAc)_2]_2•2H_2O$ was examined by EPR (Figure 2). The fluid solution EPR spectrum of $[Cu(OAc)_2]_2•2H_2O$ in MeCN only shows a minor trace of a monocopper(II) species, with the paddlewheel structure intact in solution as evinced by a frozen solution spectrum (150 K) that is characteristic of the $S = 1$ complex.[14] Treatment of $[Cu(OAc)_2]_2•2H_2O$ with piperidine (**12**) immediately results in a deep blue solution. EPR confirmed the dissociation of the paddlewheel dimer to a mononuclear species: the characteristic four-line signal resulting from the hyperfine coupling of the $S = {}^1/_2$ Cu(II) d^9 centre with its nuclear spin $I = {}^3/_2$ of the ^{63,65}Cu isotopes (100% abundant). A similar effect is exhibited upon treatment of $[Cu(OAc)_2]_2•2H_2O$ with aniline (**14**); however, the effect is notably weaker, only becoming significant at increased [**14**]. In contrast to the effect of the amine, treatment of the paddlewheel dimer with only organoboron compounds **11a** or **11b** gave no observable change to the EPR spectrum.

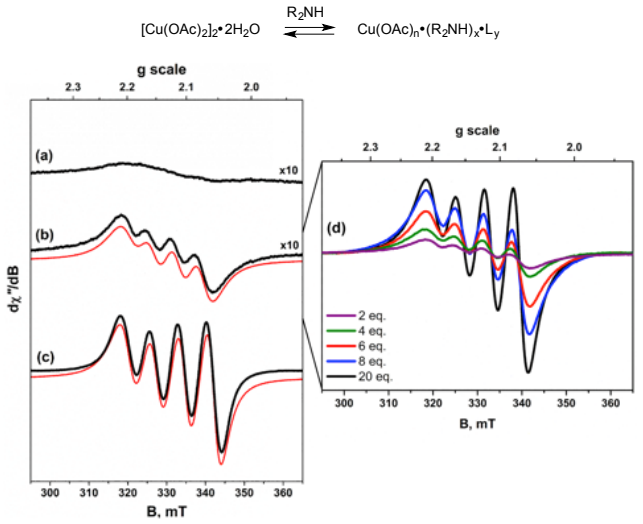

Figure 2. X-band EPR spectrum of $[Cu(OAc)_2]_2•2H_2O$ (a) in MeCN, after treatment with (b) **14** or (c) **12**, and (d) showing concentration effect of **14**, recorded at 293 K. Simulations of (b) and (c) are depicted by the red trace.

4.3.2 Structural Characterization of Cu(II) Complexes. Aging the Chan-Lam reaction of **12** with **11b** delivered two different diffraction-quality crystals. The hexa-acetate paddlewheel **20** is similar to $[Cu(OAc)_2]_2•2H_2O$ with AcO^- replacing H_2O at the axial sites and the resulting anionic charge balanced by piperidinium ions. The tetracopper complex **21**, contains two bridging oxo units, four bridging acetates, two terminal acetates, and four neutral piperidine ligands (Figure 3).

Independent preparation of both **20** and **21** was also possible on gram scale (Scheme 5). Treatment of $[Cu(OAc)_2]_2•2H_2O$ with piperidinium acetate in MeCN at –20 °C delivered **20** as green crystals in 11% yield, while treatment of $[Cu(OAc)_2]_2•2H_2O$ with piperidine in PhMe at room temperature provided the large blue crystals of **21** in 29% yield.[15] Both complexes were found to be stable at room temperature over a period of weeks.

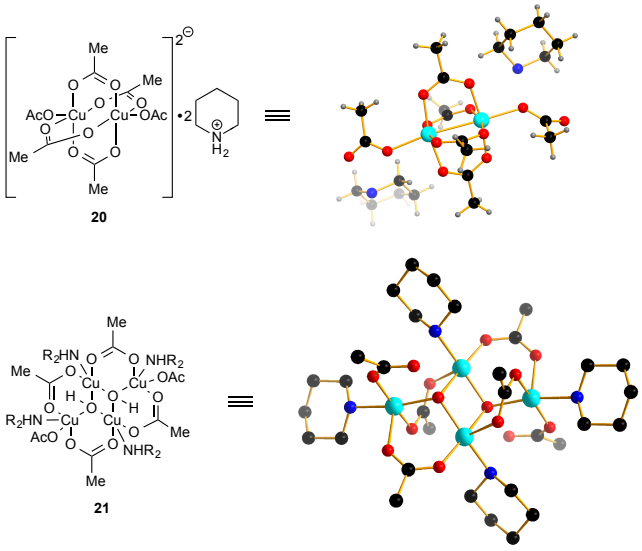

Figure 3. Isolated complexes. R_2NH = piperidine.

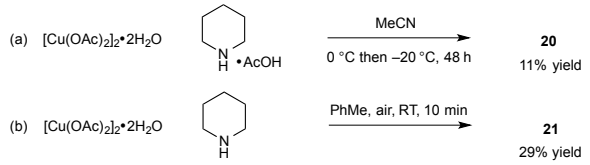

Scheme 5. Independent preparation of **20** and **21**. Isolated yields.

4.3.3 HRMS Identification of Cu(II) Complexes in Solution. High-resolution mass spectrometry (HRMS) was used to identify organometallic complexes in solution. Aliquots from the reaction of **11b** and **12** were analyzed and mass ions consistent with several proposed reaction-relevant structures were detected (Figure 4).

Two amine-ligated Cu(II) complexes, **22** and **23** (Figure 4a), were identified in relatively high abundance. The proposed structures of these two complexes are clearly related both to each other and to the tetracopper complex **21** (Figure 3). Mass ions consistent with proposed pre-transmetallation intermediate structural isomers **24** and **25** were detected (Figure 4b), as well as the corresponding proposed post-transmetallation complex **26** (Figure 4c). A $Cu(II)(Pin)_2$ complex **27** was also observed (Figure 4d).

4.4 Oxidation of Cu(I)→Cu(II). In the etherification process, Stahl has shown that oxidation of Cu(I)→Cu(II) takes place using molecular oxygen and additional Cu(I), with the requirement of acid (HX) and BX_3 (see Scheme 2).[12] The oxidation of Cu(I)OAc to $Cu(II)X_2$ under air can be readily monitored by UV-Vis spectroscopy, allowing assessment of additives (Figure 5).

Chart a shows the oxidation in the presence of specific reaction-relevant additives but in the absence of amine substrates. In the absence of any additive, CuOAc persists – no oxidation was observed by simply stirring in MeCN under air. Similarly, no oxidation was seen in the presence of Et_3N alone. However, oxidation was relatively rapid in the presence of AcOH. Oxidation was slower in the buffered system using both AcOH and Et_3N.

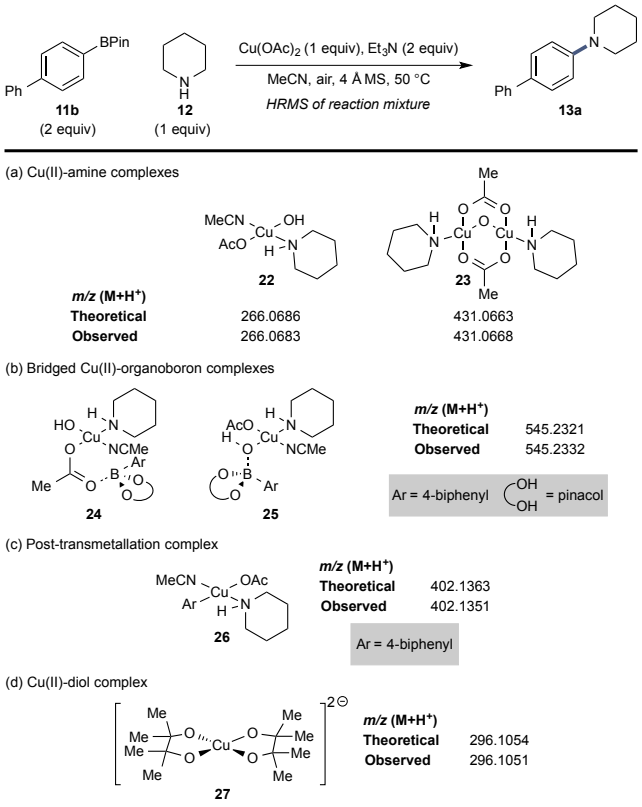

Figure 4. Proposed structures of mass ions detected by HRMS analysis of reaction mixtures.

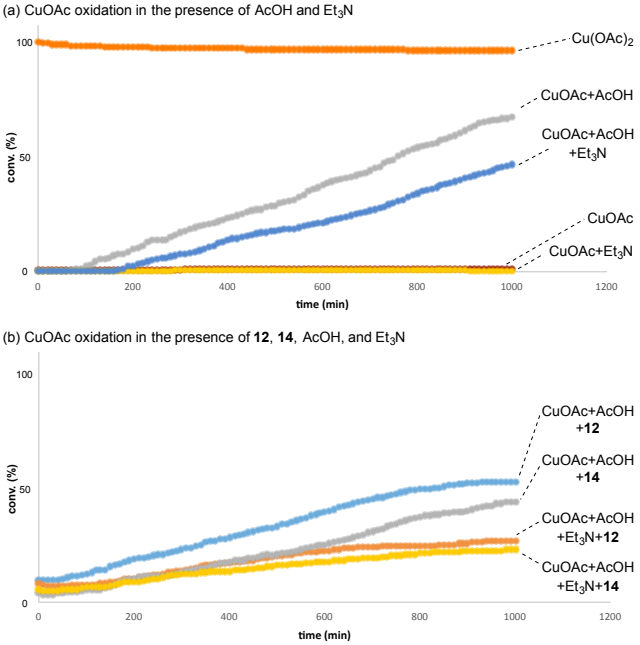

Figure 5. Oxidation of Cu(I) to Cu(II) in the presence of reaction-relevant additives monitored by UV-Vis spectroscopy. $Cu(OAc)_2$ was used as an illustrative Cu(II) reference in (a).

Similar trends were observed when the same analysis was repeated in the presence of piperidine (**12**) and aniline (**14**) (Chart b). The Cu(I) oxidation was generally more rapid in the presence of **12** than **14**, including in the presence in the presence of Et_3N, although this was marginal.

5. DISCUSSION

5.1 Organoboron Reactivity Differences and Byproduct Formation. The differences in reactivity between alkyl and aryl amines (**12** and **14**, respectively), and boronic acids and BPin esters (**11a** and **11b**, respectively) can be clearly observed in the benchmark reactions (Scheme 3). Reactions of **11a** are generally successful while those with **11b** are significantly less efficient.

With regards to byproduct formation, in the benchmark reaction of **11a** with **12** and **14** (Scheme 3 and Table 1), while formation of the desired products (**13a** and **15a**, respectively) can be excellent (*e.g.*, entries 3, 5, 8, and 10), there were several immediate observations: (1) the addition of Et_3N was beneficial, efficiency markedly improved with 1 equivalent but was optimum with 3 equivalents (*e.g.*, entries 1-3 and 5, entries 6-8 and 10). This is consistent with previous studies.[3] The improvement in yield is not due to inhibition of side reactions but rather improvement in general reactivity – starting material (**11a**) persisted in the absence of Et_3N, product distribution remained approximately constant (*e.g.*, entry 6 vs. entry 7); (2) Molecular sieves are beneficial to lower production of the oxidation product **16** (*e.g.*, entry 3 vs. entry 4, entry 8 vs. entry 9). This is consistent with the ^{18}O labeling experiments of Lam demonstrating that oxidation arises from H_2O,[4a] and observations by Evans on the effect of molecular sieves;[3b] (3) The most significant observation was the extent of the production of side products **16-18**. Oxidation can be tempered with molecular sieves but production of **16** persisted at *ca.* 5-10% while **18** varied from 12-25%. Protodeboronation was also a significant issue, with 50-68% yield of **17** generated throughout. Accordingly, even for high yielding reactions (*e.g.*, entry 5) approximately half of the total input of **11a** was consumed in side reactions, explaining the necessity for superstoichiometric quantities of **11a**. Organoboron homocoupling (Scheme 4) was found to be minimal and was not

further considered. In summary, amination is marginally competitive with side reactions under these standard conditions.

The primary goal of this study was to establish a mechanistic description of the Chan-Lam amination in order to solve these specific reactivity and byproduct formation issues, potentially allowing the development of a more general catalytic protocol for the amination of boronic acids and BPin substrates.

5.2 Entry to Catalysis. *5.2.1 Paddlewheel Dissociation, Reformation, and Reaction Inhibition.* Paddlewheel complexes are unreactive in Cu-catalyzed oxidative coupling reactions and must undergo dissociation as the first mechanistic event.[12] In etherification reactions, paddlewheel dissociation is promoted in the alcoholic media.[12,16] However, alcoholic media are not feasible in the amination reaction due to chemoselectivity issues (amination vs. etherification).[6]

EPR studies (Figure 2) demonstrated that $[Cu(OAc)_2]_2•2H_2O$ can be readily dissociated using alkyl amine **12** but less readily by aryl amine **14**. **14** was only able to induce a comparable level of dissociation of the paddlewheel when the concentration was >10 fold greater than that of **12**. This highlights an immediate reactivity difference between the amine classes (Scheme 3): dissociation of the paddlewheel dimer is dependent on Lewis basicity.

The competitive nature of this key event was reinforced by the additive experiments (Figure 1). AcOK promotes reformation of dinuclear Cu(II) species from mononuclear complexes.[12] Piperidine (**12**) induces denucleation even in the presence of additional AcOK (Figure 1, Chart b, blue line), while aniline (**14**), as a poorer ligand, does not (Figure 1, Chart b, red line), thus generating significantly less monomeric species (Scheme 6).[17]

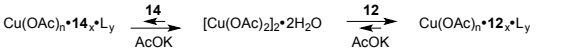

Scheme 6. Competitive vs. non-competitive denucleation of $[Cu(OAc)_2]_2•2H_2O$ with **12** and **14**.

AcOH displays a similar inhibitory effect to that of AcOK, promoting reformation of dinuclear Cu(II) species but with an additional inhibitory function. Piperidine is able to induce denucleation in the presence of AcOK (Figure 1, Chart b) but not in the presence of AcOH (Figure 1, Chart a) due to *N*-protonation, thereby necessitating the addition of a base (*e.g.*, Et_3N). Indeed, treatment of **11a** or **11b** with **20** under reaction-like conditions led to 50% and 6% yield of **13a**, respectively (Scheme 7) – less effective than standard conditions (see Scheme 3).

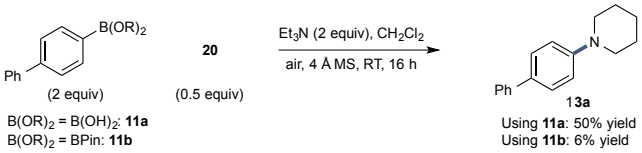

Scheme 7. Amination of **11a** and **11b** using complex **20**. Isolated yields.

In contrast, exposing **11a** or **11b** to **21** under reaction-like conditions gave **13a** in 76% and 18% yield, respectively (Scheme 8) – very similar to the typical yield for these substrates under standard conditions (87% and 28%, respectively, see Scheme 3). Unfortunately, complexes derived from **14** were not isolated preventing a similar evaluation.

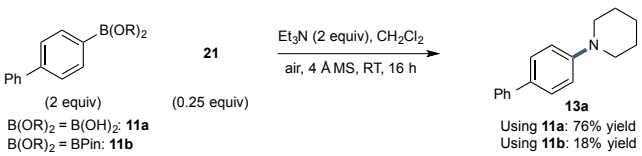

Scheme 8. Amination of **11a** and **11b** using complex **21**. Isolated yields.

These experiments indicate that one of the roles of Et_3N in Chan-Lam aminations is to sequester HX, generating sufficient amine freebase to drive denucleation of paddlewheel species and allow the formation of reactive amine-ligated Cu(II) complexes, such as **21**.

Together, these data (1) support the requirement for paddlewheel dissociation as a first key mechanistic event, (2) demonstrate that reactivity differences between amine classes begin at this initial event, and (3) provide an explanation for the reactivity increase in the presence of Et_3N.

5.2.2 Organoboron Reactivity Differences: Reaction Inhibition by Pinacol. The disparity in reactivity between **11a** and **11b** can be attributed to the presence of pinacol, which has a notable inhibitory effect on the amination reaction of **11a** using both **12** and **14**, with a greater effect on the latter (see Figure 1, Chart c).

Importantly, this inhibitory function does not appear to be driven by differences in rates of transmetallation.[18] Indeed, pinacol has an immediate inhibitory function as shown in Scheme 9. The reaction of **11a** with **14** proceeds to deliver 92% of **15a** over 16 h, with 41% conversion to **15a** over 6 h. When the reaction is allowed to take place for 6 h before addition of pinacol and then allowed a further 12 h, conversion to **15a** is commensurate with the 6 h time point.

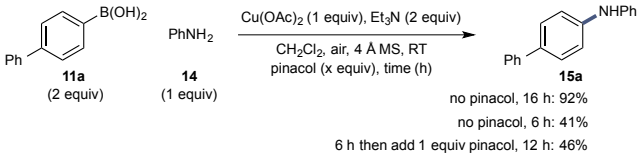

Scheme 9. Inhibition effect of pinacol. Isolated yield.

Under reaction-like conditions (without amine or $Cu(OAc)_2$), treatment of **11a** with pinacol gave 46% of **11b** over 16 h (Scheme 10). This slow esterification cannot account for the levels of inhibition observed in reactions of **11b**.

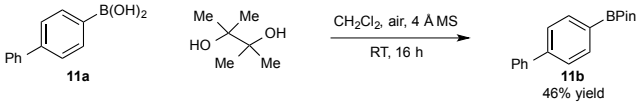

Scheme 10. Esterification of **11a** with pinacol. Determined by HPLC analysis..

This suggests that the observed inhibitory effect (Figure 1, Chart c) was not necessarily due to formation of **11b**, but rather due to some other interaction of pinacol. Various diols are known to form complexes with Cu(II), including derivatives of pinacol.[19] While a crystalline structure of a Cu(II)-pinacol complex was not obtained, NMR and HRMS analysis confirmed the presence of $Cu(II)(pinacol)_2$ **27** in solution in both isolated experiments and in samples from amination reaction mixtures using **11b** (Scheme 11). Accordingly, we believe the observed BPin reactivity issues in the Chan-Lam amination are due to catalyst inhibition by pinacol, generated either by hydrolysis of the organoboron starting material (*e.g.*, **11b**) or of the organoboron byproduct following the transmetallation event.

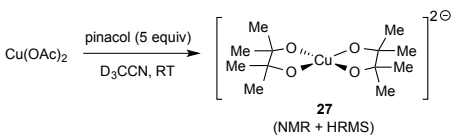

Scheme 11. Formation of $Cu(II)(pinacol)_2$ complex **27** observed by NMR and HRMS.

5.2.3 Solution Structure of the Mononuclear Cu(II) Species. Important to our goals in this study was to attempt to provide an understanding of the ligands on any Cu-based species. To achieve

this, we used a combination of HRMS analysis coupled with computational modeling. Mass ions were identified from the benchmark reactions using **11b** and **12**, and the potential structures, and their interconversion, were rationalized by modeling to assist in assembling a proposed mechanism.

Mass ions consistent with Cu(II) complex **22** and dinuclear complex **23** were identified (Figure 4). Significantly, the isolated tetracopper complex **21** appears to be a dimer of **23**, which itself is a dimer of **22** (Scheme 12). **21** is competent in the amination reaction (Scheme 8) suggesting that **21**, **22**, and **23** are in equilibrium and that **22** is the mononuclear complex produced following dissociation of $[Cu(OAc)_2]_2$•$2H_2O$ with **21** a resting state/reservoir.

In relation to the proposed structure of **22**, calculations reveal this complex and its amide isomer **28** are isoenergetic. However, we posit **22** as the likely structure based on the structure of **21** and previous observations.[20]

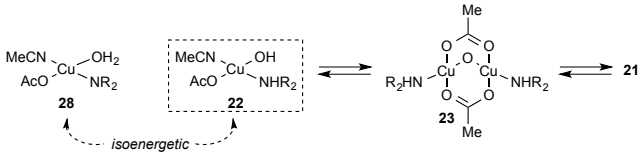

Scheme 12. Proposed structure of **22** and connection with **21** and **23**. R_2NH = piperidine.‡

5.3 Transmetallation. HRMS analysis of the **11b** reaction mixture allowed detection of mass ions consistent with proposed isostructural Cu(II) complexes **24** and **25** (Figure 4), which is consistent with a pre-transmetallation intermediate arising from ligation of **11b** to **22** (Scheme 13).

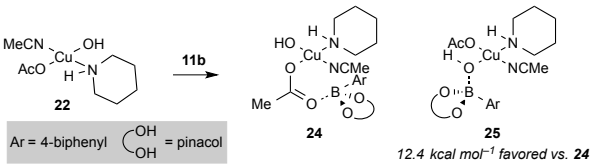

Scheme 13. Proposed generation of isostructural pre-transmetallation intermediates detected by HRMS.‡

Complex **24** is consistent with the resting state proposed by Stahl (**9**, Scheme 2);[12] however, molecular modeling of these proposed structural isomers suggests **25** was 12.4 kcal mol^{-1} more stable than **24**. Accordingly, whether or not **24** has a role is unclear. However, HRMS also allowed detection of a post-transmetallation intermediate **26** (Figure 4 and Scheme 14). In agreement with Stahl, a molecular modeling comparison of transmetallation via a 4-membered transition state beginning from **25** and the 6-membered transition state beginning from **24** favored the 4-membered transition state by 17.7 kcal mol^{-1}. The production of the expected boron byproduct, HO–BPin, could be observed by ^{11}B NMR (see ESI).

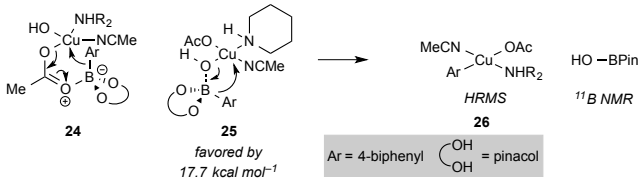

Scheme 14. Comparison of transmetallation pathways to aryl-Cu(II) species **26**. R_2NH = piperidine.‡

More holistically, a 4-membered oxo-metal transmetallation pathway is consistent with organoboron transmetallation in other transition metal-catalyzed coupling reactions. For example, within Suzuki-Miyaura cross-coupling using Pd and Ni,[21,22] and Rh-catalyzed conjugate addition.[23] Accordingly, there is potentially an elegant symmetry and generality in the transmetallation of organoboron compounds to these metal species.

5.4 Reductive Elimination: C-N vs. C-O. Based on Stahl's mechanism,[12] following transmetallation, oxidation via disproportionation generates a Cu(III) intermediate that undergoes reductive elimination to give the product and a Cu(I) species. While not detected,[24] a proposed structure of this Cu(III) intermediate **29**, based on the structure of **26**, allowed investigation of the reductive elimination event (Scheme 15).

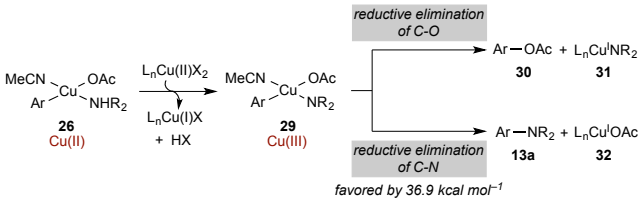

Scheme 15. Oxidation and reductive elimination. R_2NH = piperidine.‡

Computational modeling of reductive elimination from **29** also favors C-N bond formation over C-O bond formation by 36.9 kcal mol^{-1}. This is consistent with the work of Fensterbank.[20b] Accordingly, we do not believe that formation of phenol side products arises from competitive reductive elimination of **29** but from other processes (*vide infra*).

5.5 (Re)Oxidation of Cu(I). *5.5.1 Completion of the Catalytic Cycle.* Completion of the catalytic cycle requires reoxidation of Cu(I) to Cu(II). Stahl has shown that this takes place using molecular oxygen and additional Cu(I), with the requirement of acid (HX) and BX_3 (see Scheme 2).[12] As proposed above, Cu(I)OAc is the product of the reductive elimination event (Scheme 15). Evaluation of the oxidation of Cu(I)OAc to $Cu(II)X_2$ in the presence of various reaction-relevant additives was informative, highlighting the fundamental effects of the amine components (Figure 5).

The requirement for HX is consistent with our observations (Figure 5, Chart a). In the presence of only Et_3N, no oxidation takes place and in the presence of AcOH, oxidation is relatively rapid. With both AcOH and Et_3N, oxidation proceeds more slowly. When the same analysis is repeated in the presence of piperidine (**12**) and aniline (**14**) (Figure 5, Chart b), the same trends are observed but, notably, the Cu(I) oxidation is more rapid in the presence of **12** than **14**, highlighting a second difference between the amine classes.[25] Oxidation was comparably slow for both amines in the presence of Et_3N.

These observations point to two fundamental roles for Et_3N: (1) to sequester AcOH in order to avoid (re)formation of inactive paddlewheel complexes (*e.g.*, **20**) and (2) the resulting salt (Et_3N•AcOH) provides the necessary H^+ to promote Cu(I) oxidation. This promotes reaction efficiency consistent with previous observations.[3] Similarly, the amine substrates have two essential roles beyond acting as the coupling partner: (1) to induce dissociation of paddlewheel complexes and (2) to promote Cu(I) oxidation. That oxidation is more rapid in the presence of **12** vs. **14** indicates that oxidation takes place from an amine-ligated Cu(I) complex. This, then, allows access directly to Cu(II) complex **22** (Scheme 16).

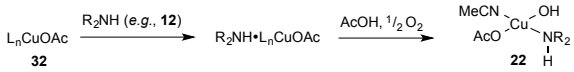

Scheme 16. Oxidation of Cu(I)→Cu(II).

5.5.2 Cu(I) and Byproduct Generation. The (re)oxidation event of Cu(I) to Cu(II) has important ramifications on amination reaction performance, specifically with respect to by-product generation. Oxidation to deliver **16** and protodeboronation to deliver **17** are problematic and both of these processes are known to

be facilitated by Cu(I) species more than Cu(II).[26] Indeed, treatment of **11a** with CuOAc delivers 40% oxidation (**16**) and 56% protodeboronation (**17**) while the corresponding reaction with $Cu(OAc)_2$ gives 9% and 63%, respectively (Scheme 17). Accordingly, we believe that oxidation issues arise primarily through the side reactions of Cu(I)X species generated after reductive elimination prior to reoxidation to Cu(II). Protodeboronation was equally problematic for both Cu(I) and Cu(II) in these control experiments. However, additional data (*vide infra*) suggests that protodeboronation takes place when the reaction is unable to take any alternative course (*e.g.*, amination), such as in this control reaction. Consequently, we believe that a slow Cu(I)→Cu(II) oxidation will lead to increased levels of side reactions.

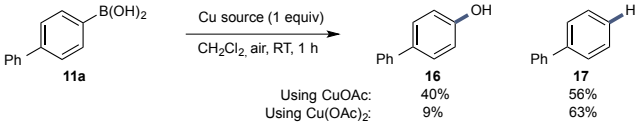

Scheme 17. Comparison of Cu(I) vs. Cu(II) on oxidation/protodeboronation of **11a**. Determined by HPLC analysis.

5.6 Proposed Mechanism for the Chan-Lam Amination. Based on previous work by Stahl on the etherification process,[12] and the isolated stoichiometric experiments detailed above, a complete mechanistic description of the Chan-Lam amination can be proposed (Scheme 18).

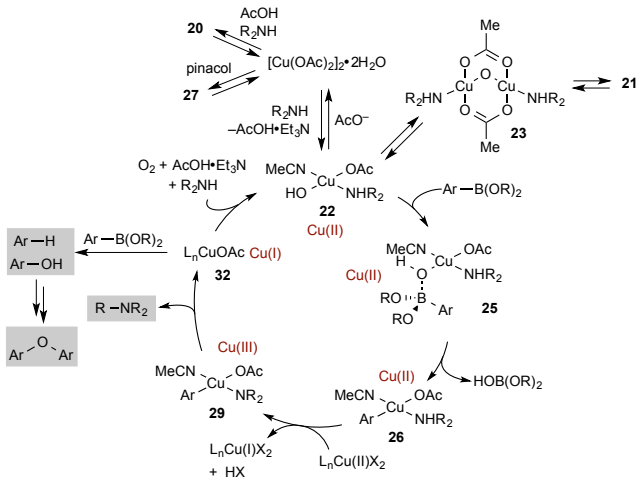

Scheme 18. Proposed mechanism of the Chan-Lam amination.

$[Cu(OAc)_2]_2$•$2H_2O$ undergoes denucleation by action of the amine to a mononuclear Cu(II) complex **22**, which exists in equilibrium with its dimer, **23**, and tetramer, **21**, derivatives. This initial amine-driven denucleation event is essential to catalysis and can be inhibited by action of AcO^- and AcOH, both of which promote reformation of paddlewheel species. AcOH simultaneously inhibits denucleation by protonation of the amine, giving the hexa-acetate paddlewheel **20**. Engagement of the organoboron component leads to transmetallation via 4-membered transition state **25** to deliver Cu(II) species **26**. Oxidation to Cu(III) via disproportionation gives complex **29**. A selective C-N reductive elimination liberates the desired amine product and a Cu(I)OAc species **32**. Completion of the catalytic cycle is achieved via oxidation to Cu(II) in the presence of O_2 and HX and is promoted in the presence of the amine substrate. Side product generation is a function of this reoxidation event: a slow oxidation provides sufficient opportunity for Cu(I)-promoted oxidation and protodeboronation.

The origin of substrate reactivity issues has been identified: (1) the reactivity issue of aryl amines (*e.g.*, **14**) compared to their alkyl counterparts (*e.g.*, **12**) is a function of the Lewis basicity – decomplexation of the paddlewheel dimer is more readily achieved with **12** vs. **14**. In addition, the reoxidation event from Cu(I) to Cu(II) is slower with **14** vs. **12**. (2) BPin substrates are problematic due to catalyst inhibition by pinacol (generating **27**) produced as a byproduct during the reaction.

5.7 Development of a General Chan-Lam Amination. Based on the above discussion, there are three key events that must be controlled to resolve the substrate reactivity and side product issues associated with the Chan-Lam amination: (1) sequestration of AcO^-/AcOH; (2) removal of free pinacol; and (3) promotion of Cu(I) oxidation. These are not intuitively/simply solved since AcOH is both beneficial and inhibitory (*vide supra*). However, based on our previous work,[27] a straightforward solution was offered using a byproduct of the Chan-Lam amination, boric acid, in combination with inverting the conventional organoboron:amine stoichiometry.

$B(OH)_3$ reversibly forms borates with AcO^-/AcOH and forms stable boric acid esters with diols, including pinacol (Scheme 19a).[28] Control experiments also demonstrated that $B(OH)_3$ promotes oxidation of Cu(I) to Cu(II) more effectively than **12**/**14** in the presence of AcOH and Et_3N (Scheme 19b vs. Figure 5).

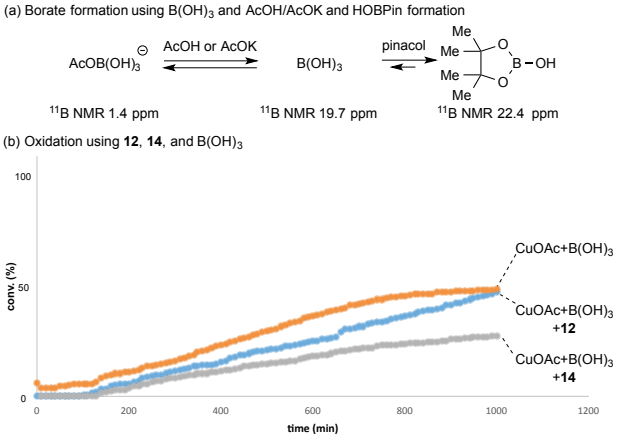

Scheme 19. (a) Reversible borate formation with $B(OH)_3$ and AcOH/AcO^-. Determined by ^{11}B NMR. (b) Cu(I) oxidation using $B(OH)_3$ determined by UV-Vis spectroscopy.

In addition, based on the findings above, Cu(I) oxidation is dependent on [amine]. Increasing [amine] would be expected to facilitate Cu(I) oxidation and lower byproduct generation. Increased [amine] would also have a second beneficial effect by driving denucleation of paddlewheel complexes.

This simple change in stoichiometry was found to be effective, leading to a significant improvement in reaction profile – yield of desired product increased while overall byproduct generation was decreased (Scheme 20).

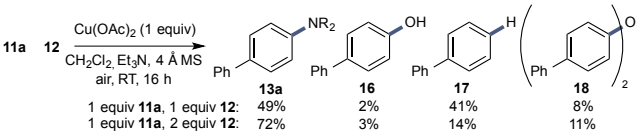

Scheme 20. Impact of amine stoichiometry on side product formation. Determined by HPLC analysis using an internal standard.

Based on all of this, in the context of the Chan-Lam reaction using stoichiometric $Cu(OAc)_2$, upon replacing the conventional organic base (Et_3N) directly with $B(OH)_3$ and inverting the organoboron:amine stoichiometry, the Chan-Lam amination can be improved considerably (Scheme 21). On comparison with the reaction profile shown in Scheme 3c, a dramatic improvement in product distribution is apparent and in a significantly improved timeframe (2 h vs. 16 h).

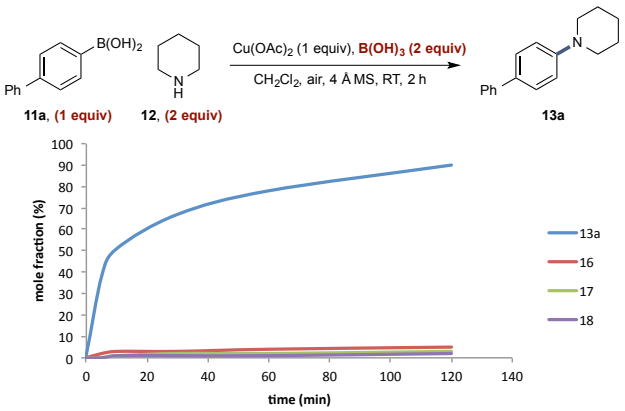

Scheme 21. Reaction profile for the $B(OH)_3$-promoted Chan-Lam amination. Determined by HPLC analysis..

More importantly, we have found that the use of $B(OH)_3$ as a promoter could be used to allow the development of a generally effective catalytic Chan-Lam amination of aryl BPin that was broadly effective for both alkyl and aryl amines (Scheme 22a and 22b, respectively; see ESI for optimization).[29] Comparable levels of efficiency were noted for BPin vs. boronic acid as well as catalytic *vs.* stoichiometric $Cu(OAc)_2$ (see **13a** and **15a**). The same reaction conditions were also effective within etherification and thiolation (Scheme 22c). It should be noted that while these conditions operate effectively across reaction partners of broadly varied electronic and structural variety, *ortho*-substitution on the aryl component generally results in poorer yields when using secondary or bulky primary amines, for example, the yield of **13g** was notably lower than that of **13o** and **13r**.

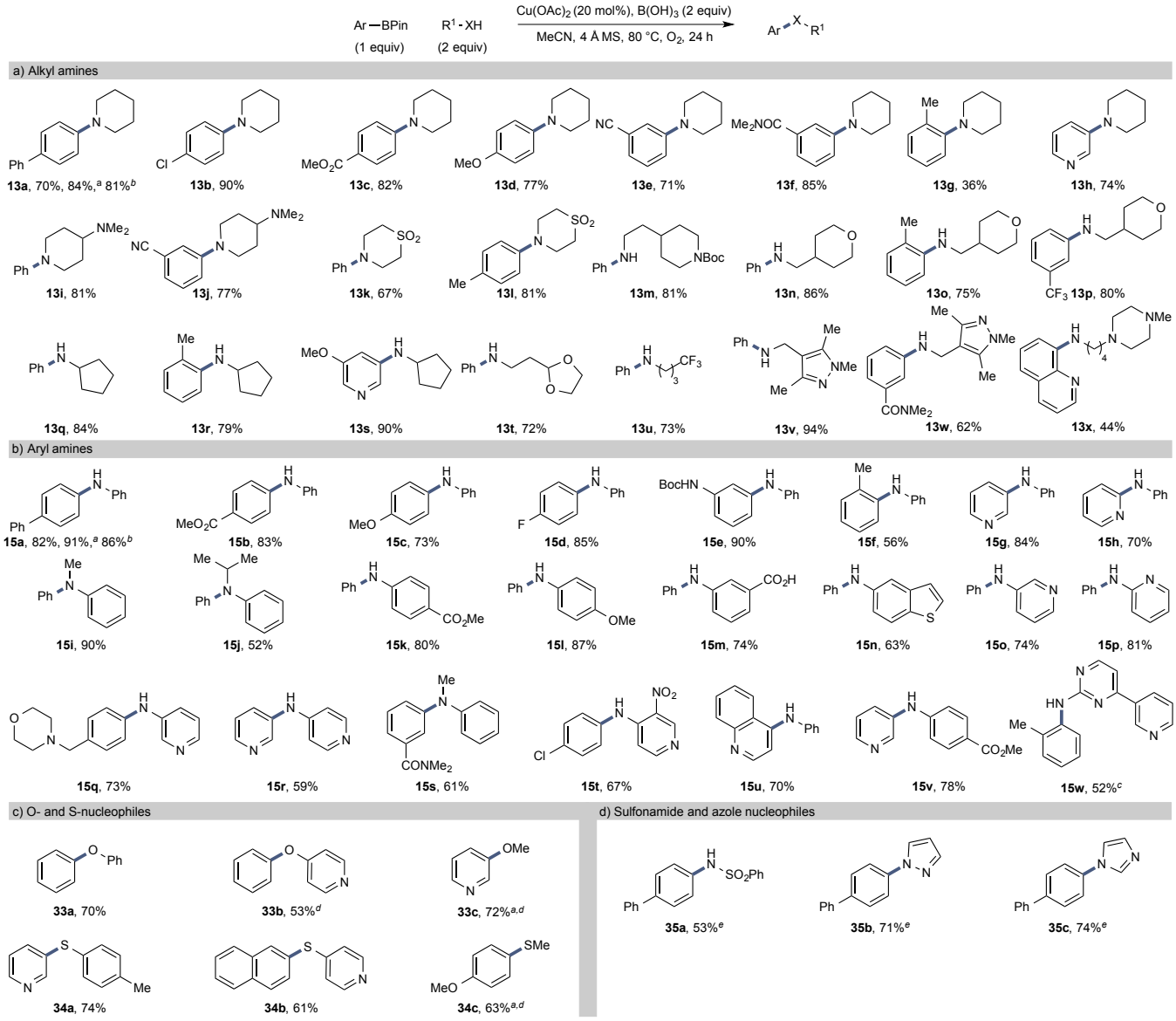

Scheme 22. $B(OH)_3$-promoted catalytic Chan-Lam reaction of ArBPin: Application. Isolated yields using FlashMaster® purification system. [a] Using 1 equiv. $Cu(OAc)_2$ under air. [b] Using the equivalent boronic acid. [c] Using DMSO as solvent. [d] Using 3 equiv. of the alcohol/sulfide. [e] Using 1.3 equiv of the azole/sulfonamide.

To further validate the applicability of our developed method on a molecule of higher molecular weight and increased functionality, we assessed the developed reaction conditions within the synthesis of the tyrosine-kinase inhibitor Imatinib (Gleevec®, **41**, Scheme 19).[30] Formation of the required BPin compound was achieved over three steps via an acylation/alkylation sequence

using dichloride **36** and amines **37** and **38**. Subsequent Miyaura borylation of **39** gave BPin **40**. Application of the developed reaction conditions towards Chan-Lam amination of **40** gave access to **41** in 67% isolated yield on 0.5 g scale.

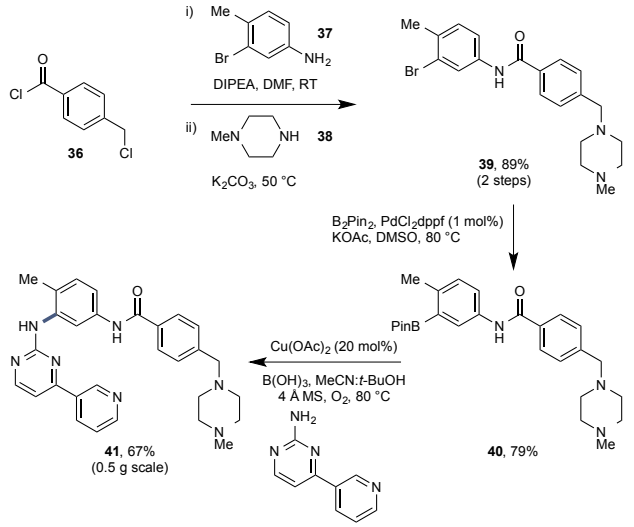

Scheme 23. Synthesis of Imatinib using the $B(OH)_3$-promoted catalytic Chan-Lam amination. Isolated yields.

6. CONCLUSIONS

In summary, investigation of the Chan-Lam amination has allowed a complete mechanistic description to be assembled. Spectroscopic analyses have provided insight into the course of the reaction with a formative identification of key reactive intermediates. This has allowed the origin of three specific issues (BPin reactivity, aryl amine reactivity, and side reactions (oxidation, protodeboronation)) to be determined. In addition, synergistic promotive effects of boric acid were identified and have been leveraged to overcome these issues, providing the first generally efficient BPin Chan-Lam amination conditions proceeding under non-basic reaction conditions. We believe these findings will allow more general uptake and application of this valuable C-N bond forming reaction.

ASSOCIATED CONTENT

Supporting Information

Experimental procedures, assay details and spectra, characterization data for all compounds. The Supporting Information is available free of charge on the ACS Publications website.

AUTHOR INFORMATION

Corresponding Author

* allan.watson.100@strath.ac.uk

Author Contributions

The manuscript was written through contributions of all authors.

ACKNOWLEDGMENT

This work was supported by the EPSRC. We thank the EPSRC and GlaxoSmithKline (GSK) for a PhD studentship (JCV) and GlaxoSmithKline for financial support and chemical resources. We thank the analytical team at GSK for assistance with HRMS analysis. We thank the Reviewers for helpful advice during the submission of this manuscript.

ABBREVIATIONS

EPR, electron paramagnetic resonance; HPLC, high performance liquid chromatography; NMR, nuclear magnetic resonance; Pin, pinacolato; RT, room temperature.

REFERENCES

‡ Modeled at the B3LYP/def2-TZVP level of theory with solvent effects included using COSMO. *cis/trans* isomers were evaluated but were isoenergetic within the experimental limits. See SI for full details.

[1] For a recent review, see: Bariwal, J.; Van der Eycken, E. *Chem. Soc. Rev.* **2013**, *42*, 9283−9303.
[2] For reviews, see: (a) Hassan, J.; Sévignon, M.; Gozzi, C.; Schulz, E.; Lamaire, M. *Chem. Rev.* **2002**, *102*, 1359–1470; (b) Sambiagio, C.; Marsden, S. P.; Blacker, A. J.; McGowan, P. C. *Chem. Soc. Rev.* **2014**, *43*, 3525–3550.
[3] (a) Chan, D. M. T.; Monaco, K. L.; Wang, R. P.; Winters, M. P. *Tetrahedron Lett.* **1998**, *39*, 2933−2936; (b) Evans, D. A.; Katz, J. L.; West, T. R. *Tetrahedron Lett.* **1998**, *39*, 2937−2940; (c) Lam, P. Y. S.; Clark, C. G.; Saubern, S.; Adams, J.; Winters, M. P.; Chan, D. M. T.; Combs, A. *Tetrahedron Lett.* **1998**, *39*, 2941–2944.
[4] For reviews, see: (a) Qiao, J.; Lam, P. Y. S. Synthesis **2011**, 829–856; (b) Lam, P. Y. S. Chan–Lam Coupling Reaction: Copper-promoted C–Element Bond Oxidative Coupling Reaction with Boronic Acids In Synthetic Methods in Drug Discovery: Volume 1, Eds.: Blakemore, D. C.; Doyle, P. M.; Fobian, Y. M., Royal Society of Chemistry: Cambridge, **2016**, Chapter 7, p 242–273.
[5] For selected examples, see: (a) Fan, M.; Zhou, W.; Jiang, Y.; Ma, D. *Angew. Chem. Int. Ed.* **2016**, *55*, 6211–6215; (b) Zhou, W.; Fan, M.; Yin, J.; Jiang, Y.; Ma, D. *J. Am. Chem. Soc.* **2015**, *137*, 11942−11945.
[6] Vantourout, J. C.; Law, R. P.; Isidro-Llobet, A.; Atkinson, S. J.; Watson, A. J. B. *J. Org. Chem*. **2016**, *81*, 3942–3950.
[7] For examples, see: Hall, D. G. Structure, Properties, and Preparation of Boronic Acid Derivatives In Boronic Acids: Preparation and Applications in Organic Synthesis and Medicine; Hall, D. G., Ed., Wiley-VCH: Weinheim, **2005**; Chapter 1, p 1–133.
[8] For selected examples, see: (a) Larsen, M. A.; Wilson, C. V.; Hartwig, J. F. *J. Am. Chem. Soc.* **2015**, *137*, 8633–8643; (b) Larsen, M. A.; Hartwig, J. F. *J. Am. Chem. Soc.* **2014**, *136*, 4287–4299; (c) Cho, J.-Y.; Tse, M. K.; Holmes, D.; Maleczka, R. E.; Smith, M. R. *Science* **2002**, *295*, 305–308; (d) Ishiyama, T.; Takagi, J.; Ishida, K.; Miyaura, N.; Anastasi, N. R.; Hartwig, J. F. *J. Am. Chem. Soc.* **2002**, *124*, 390–391; (e) Ishiyama, T.; Murata, M.; Miyaura, N. *J. Org. Chem.* **1995**, *60*, 7508–7510.
[9] For an authoritative study, see: Cox, P. A.; Leach, A. G.; Campbell, A. D.; Lloyd-Jones, G. C. *J. Am. Chem. Soc.* **2016**, *138*, 9145–9157.
[10] For examples, see: (a) Tzschucke, C.; Murphy, J.; Hartwig, J. F. *Org. Lett.* **2007**, *9*, 761−764; (b) Sueki, S.; Kuninobu, Y. *Org. Lett.* **2013**, *15*, 1544−1547; (c) McGarry, K. A.; Duenas, A. A.; Clark, T. B. *J. Org. Chem.* **2015**, *80*, 7193−7204; (d) Marcum, J. S.; McGarry, K. A.; Ferber, C. J.; Clark, T. B. *J. Org. Chem.* **2016**, *8*, 7963–7969.
[11] For previous discussions of amination mechanisms in several different contexts, see: (a) Collman, J. P.; Zhong, M. *Org. Lett.* **2000**, *2*, 1233–1236; (b) Collman, J. P.; Zhong, M.; Zhang, C.; Constanzo, S. *J. Org. Chem.* **2001**, *66*, 7892–7897; (c) Lam, P. Y. S.; Bonne, D.; Vincent, G.; Clark, C. G.; Combs, A. P. *Tetrahedron Lett.* **2003**, *44*, 1691–1694; (d) Tromp, M.; van Strijdonck, G. P. F.; van Berkel, S. S.; van den Hoogenband, A.; Feiters, M. C.; de Bruin, B.; Fiddy, S. G.; van der Eerden, A. M. J.; van Bokhoven, J. A.; van Leeuwen, P. W. N. M.; Koningsberger, D. C. *Organometallics* **2010**, *29*, 3085–3097; (e) Liu, C.-Y.; Li, Y.;

Ding, J.-Y.; Dong, D.-W.; Han, F.-S. *Chem. Eur. J.* **2014**, *20*, 2373–2381. See also ref 10b.
[12] (a) King, A. E.; Brunold, T. C.; Stahl, S. S. *J. Am. Chem. Soc.* **2009**, *131*, 5044–5045; (b) King, A. E.; Ryland, B. L.; Brunold, T. C.; Stahl, S. S. *Organometallics* **2012**, *31*, 7948–7957.
[13] For a study of organoboron homocoupling using Cu(I) and Cu(II), see: Demir, A. S.; Reis, O.; Emrullahoglu, M. *J. Org. Chem.* 2003, *68*, 10130–10134.
[14] Sharrock, P.; Melník, M. *Can. J. Chem.* **1985**, *63*, 52–56.
[15] Klein, J. E. M. N.; Thatcher, R. J.; Whitwood, A. C.; Taylor, R. J. K. *Acta Cryst.* **2011**, *C67*, m108–m110.
[16] (a) Grasdalen, H.; Svare, I. *Acta Chem. Scand.* **1971**, *25*, 1089−1102; (b) Rao, V. M.; Sathyanarayana, D. N.; Manohar, H. *Indian J. Chem.* **1985**, *24*, 417−418.
[17] The formation of aniline-Cu(II) complexes derived from $[Cu(OAc)_2]_2•2H_2O$ is typically achieved in alcoholic solvents (*e.g.*, MeOH) in order to provide sufficient mononuclear $Cu(OAc)_2$ (see ref 16). For example, see: (a) Van Heuvelen, A.; Goldstein, L. *J. Phys. Chem.* **1968**, *72*, 481–485. In contrast, alkyl amine complexes of are more readily formed. For example, see: (b) Narain, G. *Can. J. Chem.* **1965**, *44*, 895–898.
[18] No data was captured regarding transmetallation rates. For examples of BPin esters undergoing slower transmetallation than boronic acids in Pd catalysis, see: (a) Carrow, B. P.; Hartwig, J. F. *J. Am. Chem. Soc.* **2011**, *133*, 2116–2119; (b) Fyfe, J. W. B.; Fazakerley, N. J.; Watson, A. J. B. *Angew. Chem. Int. Ed.* **2017**, *56*, 1249–1253.
[19] For examples of Cu(II)-diol complexes, see: (a) Laleh Tahsini, L.; Specht, S. E.; Lum, J. S.; Nelson, J. J. M.; Long, A. F.; Golen, J. A.; Rheingold, A. L.; Doerrer, L. H. *Inorg. Chem.* **2013**, *52*, 14050−14063; (b) Sillanpää, R. *Inorg. Chim. Acta* **1984**, *82* ,75−80.
[20] (a) Jones, G. O.; Liu, P.; Houk, K. N.; Buchwald, S. L. *J. Am. Chem. Soc.* **2010**, *132*, 6205–6213; (b) Jacquet, J.; Chaumont, P.; Gontard, G.; Orio, M.; Vezin, H.; Blanchard, S.; Desage-El Murr, M.; Fensterbank, L. *Angew. Chem. Int. Ed.* **2016**, *55*, 10712–10716.
[21] For discussions of oxo-Pd transmetallation, see: (a) Carrow, B. P.; Hartwig, J. F. *J. Am. Chem. Soc.* **2011**, *133*, 2116–2119; (b) Amatore, C.; Jutand, A.; Le Duc, G. *Chem. Eur. J.* **2011**, *17*, 2492–2503; (c) Schmidt, A. F.; Kurokhtina, A. A.; Larina, E. V. *Russ. J. Gen. Chem.* **2011**, *81*, 1573–1574; (d) Wei, C. S.; Davies, G. H. M.; Soltani, O.; Albrecht, J.; Gao, Q.; Pathirana, C.; Hsiao, Y.; Tummala, S.; Eastgate, M. D. *Angew. Chem. Int. Ed.* **2013**, *52*, 5822–5826; (e) Thomas, A. A.; Denmark, S. E. *Science* **2016**, *352*, 329–332.
[22] For a discussion of oxo-Ni transmetallation, see: Christian, A. H.; Müller, P.; Monfette, S. *Organometallics* **2014**, *33*, 2134–2137.
[23] For a discussion of oxo-Rh transmetallation, see: Hayashi, T.; Takahashi, M.; Takaya, Y.; Ogasawara, M. *J. Am. Chem. Soc.* **2002**, *124*, 5052–5058.
[24] Detection of Cu(III) by HRMS: Putau, A.; Brand, H. Koszinowski, K. *J. Am. Chem. Soc.* **2012**, *134*, 613–622.
[25] For a discussion of Cu(I)/Cu(II) redox processes, see: McCan, S. D.; Stahl, S. S. *Acc. Chem. Res.* **2015**, *48*, 1756–1766.
[26] For example, see: Chu, L.; Qing, F.-L. *Org. Lett.* 2010, *12*, 5060–5063.
[27] (a) Fyfe, J. W. B.; Seath, C. P.; Watson, A. J. B. *Angew. Chem. Int. Ed.* **2014**, *53*, 12077−12080; (b) Molloy, J. J.; Law, R. P.; Fyfe, J. W. B.; Seath, C. P.; Hirst, D. J.; Watson, A. J. B. *Org. Biomol. Chem.* **2015**, *13*, 3093−3102; (c) Fyfe, J. W. B.; Valverde, E.; Seath, C. P.; Kennedy, A. R.; Anderson, N. A.; Redmond, J. M.; Watson, A. J. B. *Chem. Eur. J.* **2015**, *21*, 8951−8964; (d) Seath, C. P.; Fyfe, J. W. B.; Molloy, J. J.; Watson, A. J. B. *Angew. Chem. Int. Ed.* **2015**, *54*, 9976−9979; (e) Muir, C. W.; Vantourout, J. C.; Isidro-Llobet, A.; Macdonald, S. J. F.; Watson, A. J. B. *Org. Lett.* **2015**, *17*, 6030–6033; (f) Molloy, J. J.; Clohessy, T. A.; Irving, C.; Anderson, N. A.; Lloyd-Jones, G. C.; Watson, A. J. B. *Chem. Sci.* **2017**, *8*, 1551–1559; (g) Fyfe, J. W. B.; Fazakerley, N. J.; Watson, A. J. B. *Angew. Chem. Int. Ed.* **2017**, *56*, 1249−1253.
[28] For a discussion, see ref 27c and references therein.
[29] It should be noted that $B(OH)_3$ was also found to promote speciation equilibria with **11b**, but this was found to be rather slow under the reaction conditions (see ESI).
[30] CAS Registry Number: 152459-95-5.

Insert Table of Contents artwork here